

Virion Incorporation of the Herpes Simplex Virus Type 1 Tegument Protein VP22 Occurs via Glycoprotein E-Specific Recruitment to the Late Secretory Pathway[∇]

Julianna Stylianou,¹† Kevin Maringer,¹† Rachelle Cook,² Emmanuelle Bernard,² and Gillian Elliott^{1,2*}

Department of Virology, Faculty of Medicine, Imperial College London, London, United Kingdom,¹ and Marie Curie Research Institute, Oxted, Surrey, United Kingdom²

Received 12 January 2009/Accepted 26 February 2009

The mechanism by which herpesviruses acquire their tegument is not yet clear. One model is that outer tegument proteins are recruited by the cytoplasmic tails of viral glycoproteins. In the case of herpes simplex virus tegument protein VP22, interactions with the glycoproteins gE and gD have been shown. We have previously shown that the C-terminal half of VP22 contains the necessary signal for assembly into the virus. Here, we show that during infection VP22 interacts with gE and gM, as well as its tegument partner VP16. However, by using a range of techniques we were unable to demonstrate VP22 binding to gD. By using pulldown assays, we show that while the cytoplasmic tails of both gE and gM interact with VP22, only gE interacts efficiently with the C-terminal packaging domain of VP22. Furthermore, gE but not gM can recruit VP22 to the Golgi/trans-Golgi network region of the cell in the absence of other virus proteins. To examine the role of the gE-VP22 interaction in infection, we constructed a recombinant virus expressing a mutant VP22 protein with a 14-residue deletion that is unable to bind gE (Δ gEbind). Coimmunoprecipitation assays confirmed that this variant of VP22 was unable to complex with gE. Moreover, VP22 was no longer recruited to its characteristic cytoplasmic trafficking complexes but exhibited a diffuse localization. Importantly, packaging of this variant into virions was abrogated. The mutant virus exhibited poor growth in epithelial cells, similar to the defect we have observed for a VP22 knockout virus. These results suggest that deletion of just 14 residues from the VP22 protein is sufficient to inhibit binding to gE and hence recruitment to the viral envelope and assembly into the virus, resulting in a growth phenotype equivalent to that produced by deleting the entire reading frame.

The herpesvirus tegument is the virion compartment located between the DNA-containing capsid and the virus envelope (6). Although it is well defined that the viral capsid assembles in the nucleus (37, 38) and the viral envelope is acquired from cellular membranes (3, 24), the mechanism of tegument protein acquisition is still to be established. At least 20 virus-encoded components are recruited into the herpes simplex virus type 1 (HSV-1) tegument (32), and there is increasing evidence to suggest that subsets of these proteins may be added as assembly progresses along the maturation pathway (28). To ensure efficient incorporation, it is likely that individual tegument proteins are specifically targeted to their cellular site of recruitment. Such targeting could involve interaction with a viral partner, a cellular partner, or both. A clearer understanding of how individual tegument proteins are acquired by newly assembling virions will help to define the herpesvirus assembly pathway.

A number of protein-protein interactions between individual tegument proteins (13, 40, 42), and between tegument proteins and glycoproteins (19, 20, 22, 32), have been described that may provide useful insight into the assembly process. In particular, the interaction of tegument proteins with the cytoplas-

mic tails of virus glycoproteins provides an attractive mechanism for the virion recruitment of at least the outer components of the tegument. In the case of VP22, the homologues from pseudorabies virus (PRV) and HSV-1 have been shown to interact with the cytoplasmic tail of gE (19, 20, 32). However, the role of this interaction in virus infection has not yet been clearly defined and the fact that additional glycoprotein interactions have been described, with gM in the case of PRV and gD in the case of HSV-1, may point to potential redundancy in the mechanism of VP22 packaging (4, 19, 20). In addition, we and others have previously shown that HSV-1 VP22 interacts directly with a second tegument protein, namely, VP16 (13, 33), an interaction that could provide an alternative route for VP22 to enter the virion. In a previous study, we concluded that the region of VP22 containing its VP16 interaction domain was required but not sufficient for optimal VP22 packaging into the assembling virion, with an additional C-terminal determinant also involved (23). We also demonstrated that the same region of VP22 that was required for virion packaging was essential to target the protein to its characteristic cytoplasmic trafficking complexes, suggesting that these specific sites may be the location in the cell for VP22 assembly into the virion (23). Since that study, O'Regan and coworkers have reported that the C-terminal half of HSV-1 VP22 also contains the binding site for gE (32), providing a possible candidate for an additional VP22 binding partner. Furthermore, as HSV-1 VP22 has been shown to bind to gD and PRV VP22 interacts with gM, it is possible that the C terminus of VP22 contains a gD and/or a gM binding site (4, 20).

* Corresponding author. Mailing address: Department of Virology, Faculty of Medicine, Imperial College London, London, United Kingdom. Phone: 44 0207 594 5037. Fax: 44 0207 594 3973. E-mail: g.elliott@imperial.ac.uk.

† Both authors contributed equally to this work.

[∇] Published ahead of print on 11 March 2009.

In the present study, we aimed to clarify the molecular mechanism by which VP22 is recruited into the virus particle. We show that HSV-1 VP22 binds efficiently to VP16, gE, and gM in the infected cell, but we cannot detect an interaction with gD. We show that the packaging domain of VP22 binds to the cytoplasmic tail of gE but not gM and that the same region of VP22 is recruited to the secretory pathway by gE in the absence of other virus proteins. Finally, we show that a mutant VP22 protein lacking a 14-residue peptide from its packaging domain is unable to interact with gE during infection, exhibits a different subcellular localization, and fails to assemble into the virus particle. This is the first characterization of a single protein-protein interaction essential for the packaging of an HSV-1 tegument protein.

MATERIALS AND METHODS

Cells. Vero, BHK, COS-1, and MDBK cells were grown in Dulbecco's modified Eagle's medium supplemented with 10% newborn calf serum. Sf9 cells were grown at 25°C in TC 100 medium (Gibco) supplemented with 10% heat-inactivated fetal bovine serum.

Plasmids and viruses. Viruses were routinely grown in BHK cells or Vero cells and titrated on Vero cells. Extracellular virions were purified on Ficoll gradients from the infected cell medium of 5×10^8 BHK cells as described previously (17). Infectious virus DNA was also produced from extracellular virus as described previously (17). The parental virus strain used in this study was strain 17 of HSV-1. The recombinant HSV-1 expressing green fluorescent protein (GFP)-tagged VP22 (166v) has been described previously (17). The HSV-1 VP22 deletion mutant (169v) has also been described before (12). Plasmids expressing GST fused to the C-terminal 106 residues of glycoprotein E (gE) and the C-terminal 126 residues of gM were kindly provided by Colin Crump (Department of Pathology, University of Cambridge). The expression vector for GST-full-length VP16 was kindly provided by Peter O'Hare (Marie Curie Research Institute, Oxted, Surrey, United Kingdom). Plasmids expressing gE and gM under the control of the human cytomegalovirus (CMV) immediate-early promoter were kindly provided by Helena Browne and Colin Crump, respectively (Department of Pathology, University of Cambridge). Plasmid pGE155, expressing GFP-tagged VP22 under the control of the CMV immediate-early promoter, has been described before (16). Plasmids pAM8, pAM17, pAM5, pGFP160-301, pGE171, and pGE192, expressing residues 1 to 160, 1 to 212, 1 to 267, 160 to 301, 174 to 301, and 192 to 301 of VP22 as GFP fusion proteins, have been described previously (26). Plasmid pGE197, expressing residues 1 to 226 of VP22 as a GFP fusion protein, was constructed by PCR amplification of this region of VP22, followed by insertion into pEGFPc1. Plasmid pGE198, expressing VP22 with a deletion of residues 213 to 226, was generated by PCR amplification of residues 226 to 301 of VP22 as an NsiI/BglII fragment. This fragment was then inserted into NsiI/BamHI-digested pUL49epB (35), generating a VP22 open reading frame with an internal deletion of residues 213 to 226. This open reading frame was then transferred to pEGFPc1 to generate a GFP fusion protein. To construct plasmid pRC06, expressing GFP fused to VP22 with a deletion of residues 170 to 192, the region encoding residues 1 to 170 was amplified by PCR as a BglII/HindIII fragment and inserted into BglII/HindIII-cut pGE192. Plasmid pAM15, expressing GFP fused to VP22 with a deletion of residues 160 to 174, was made in the same way by amplifying the region encoding residues 1 to 160 of VP22 by PCR and inserting this fragment into plasmid pGE171.

To transfer the Δ 213-226 mutation into the virus, the VP22 open reading frame from pGE198 was removed as a BamHI/BglII fragment and inserted into the BamHI site of plasmid pEB1, which contains the GFP open reading frame surrounded by the flanking sequences of VP22 gene UL49. This generated plasmid pEB2. The Δ gEbind virus was constructed by cotransfection of pEB2 and infectious 169vc DNA (a nonfluorescent variant of our original Δ 22 virus) into Vero cells, and the resulting green fluorescent recombinant virus was plaque purified three times on the same cells before PCR analysis and sequencing of the mutated region of the genome. The Δ 170-192 mutation of VP22 was transferred into the virus by inserting the BsrGI/NsiI fragment from pRC06 into BsrGI/NsiI-cut plasmid pGE166. The recombinant virus (Δ gEbind2) was then isolated as described above for the Δ gEbind virus.

For virus growth curves, MDBK cells grown in a six-well plate (1×10^6 /well) were infected at a multiplicity of 0.1 in 1 ml medium per well. After 1 h (taken as 1 h postinfection), the inoculum was removed, the cells were washed with

phosphate-buffered saline (PBS), and 2 ml fresh medium was added to each well. At a range of times after infection, one well of infected cells was harvested for total virus yield and titrated on Vero cells. All plaque assays were carried out in Dulbecco's modified Eagle's medium supplemented with 2% newborn calf serum and 1% human serum (Harlan Sera-Lab).

To construct baculovirus for expression of full-length His-tagged VP22, the VP22 open reading frame from plasmid pGE109 (18) was inserted as a BglII fragment into the BglII site of plasmid pAcHLT-B (Pharmingen) and the resulting plasmid was cotransfected into Sf9 cells with Baculogold DNA (Pharmingen). Recombinant baculovirus was further amplified to produce virus stocks for the purification of His-VP22.

Expression and purification of His-tagged VP22 from baculovirus-infected Sf9 cells. Following preliminary characterization of His-VP22 expression from the recombinant baculovirus, approximately 10^8 Sf9 cells were infected at a multiplicity of 5 and harvested 3 days later. A total cell extract was made by resuspension in 100 ml of lysis buffer (50 mM NaH_2PO_4 , 300 mM NaCl, 10 mM imidazole, 1% NP-40, 0.1% Triton X-100, protease inhibitors) for 10 min on ice. After centrifugation for 20 min at $9,000 \times g$ in the cold, the supernatant was retained and incubated with 2 ml of a 50% suspension of Ni-nitrilotriacetic acid (NTA) beads (Qiagen) for 1 h at 4°C. After extensive washing in 50 mM NaH_2PO_4 -300 mM NaCl-20 mM imidazole-protease inhibitors, the beads were transferred to a column and bound material was eluted with 500- μ l aliquots of 50 mM NaH_2PO_4 -300 mM NaCl-250 mM imidazole-protease inhibitors. Samples of each were analyzed by sodium dodecyl sulfate-polyacrylamide gel electrophoresis (SDS-PAGE), followed by Coomassie blue staining, and those aliquots that contained only His-VP22 were pooled.

Pulldown of infected cell extracts on His-tagged VP22. Approximately 2×10^8 Vero cells were infected with HSV-1 strain 17 at a multiplicity of 0.1, and a total extract was made 48 h after infection by resuspension in 50 ml of lysis buffer (50 mM NaH_2PO_4 , 300 mM NaCl, 10 mM imidazole, 1% NP-40, 0.1% Triton X-100, protease inhibitors) for 10 min on ice. After centrifugation for 20 min at $9,000 \times g$ in the cold, the supernatant was precleared by incubation with 2 ml of a 50% suspension of Ni-NTA beads for 1 h at 4°C. The precleared supernatant was then incubated with 2 ml of Ni-NTA beads with bound, His-tagged VP22 for a further hour at 4°C. The beads were washed twice in 50 mM NaH_2PO_4 -300 mM NaCl-20 mM-protease inhibitors, and bound material was eluted in 10 500- μ l aliquots of 50 mM NaH_2PO_4 -300 mM NaCl-250 mM imidazole-protease inhibitors.

Expression and purification of GST-tagged proteins. GST fusion proteins were expressed in *Escherichia coli* strain BL21 by inducing a 250-ml culture with 1 mM isopropyl- β -D-thiogalactopyranoside (IPTG), followed by a further 3-h incubation. The cells were then pelleted, resuspended in 10 ml PBS containing protease inhibitors and 1 mg/ml lysozyme, and left on ice for 30 min. Following sonication, Triton X-100 was added to 1% and the extracts were incubated for a further 30 min rotating at 4°C and centrifuged at $4,000 \times g$ for 30 min at 4°C. The soluble supernatant was added to 200 μ l of a 50:50 suspension of glutathione-Sepharose beads and rotated for 1 h at 4°C, and unbound protein was washed off the beads by three washes with PBS.

Pulldown of transfected cell extracts on GST-tagged proteins. COS-1 cells in 6-cm dishes were transfected with the relevant plasmids with Lipofectamine (Invitrogen). Forty hours later, cells were washed with PBS and harvested in 1 ml of lysis buffer (50 mM Tris [pH 7.5], 200 mM NaCl, 2 mM MgCl, 1% NP-40, protease inhibitors). The samples were left on ice for 20 min and centrifuged at $12,000 \times g$ for 30 min at 4°C. A 400- μ l volume of supernatant was mixed with the relevant GST fusion protein already bound to glutathione-Sepharose beads. Following 2 to 3 h of rotation at 4°C, the beads were washed three times with lysis buffer and samples of each were analyzed by SDS-PAGE and Western blotting.

Reagents and antibodies. Monoclonal antibodies to GFP and HSV-1 major capsid protein VP5 were obtained from Clontech and Autogen Bioclear, respectively. The monoclonal anti-VP16 (LP1) and anti-gD (LP14) antibodies and the polyclonal anti-gM antibody were kindly provided by Helena Browne (Department of Pathology, University of Cambridge). Anti-VP22 polyclonal antibodies AGV031 and AV600 have been described previously (16). Monoclonal anti-gE and anti-ICP0 (11060) antibodies were kindly provided by David C. Johnson (Department of Molecular Microbiology and Immunology, Oregon Health Sciences University, Portland) and Roger Everett (MRC Virology Unit, Glasgow, Scotland), respectively. Anti-TGN46 antibody was obtained from Serotec.

SDS-PAGE. Protein samples were analyzed on 10 or 15% polyacrylamide gels and electrophoresed in Tris-glycine buffer. Following electrophoresis, gels were either stained with Coomassie blue or transferred to nitrocellulose for analysis by Western blotting. Western blots were developed with an enhanced chemiluminescence kit (Pierce).

Immunofluorescence. Cells for immunofluorescence were grown on 16-mm coverslips in individual wells of a six-well plate. Cells were fixed for 20 min in 4% paraformaldehyde, permeabilized for 10 min in PBS containing 0.5% Triton X-100, and blocked by incubation for 10 min in PBS containing 10% newborn calf serum. Primary antibody was added for 15 min of incubation in the same solution, and following extensive washing in PBS, the appropriate secondary antibody (all from Vector Labs) was added in block solution and the mixture was incubated for a further 10 min. The coverslips were then washed extensively in PBS and mounted in Vectashield containing 4',6'-diamidino-2-phenylindole (DAPI; Vector Labs). Images were acquired with a Zeiss LSM410 or LSM510 confocal microscope. The resulting images were processed with Adobe Photoshop software.

Live cell fluorescence. Vero cells for fluorescence studies were grown in two-well Lab-Tek coverglass chambers (Quadrachem Laboratories). Infections of GFP-tagged viruses were carried out at a multiplicity of 5, and images were subsequently acquired with a Zeiss LSM410 or LSM510 confocal microscope. The resulting images were processed with Adobe Photoshop software.

Immunoprecipitation assay. Vero cells grown in 6-cm dishes were infected with the relevant viruses at a multiplicity of 1. After 20 to 24 h, the cells were washed twice with PBS, solubilized in 1 ml radioimmunoprecipitation assay (RIPA) buffer (50 mM Tris [pH 7.5], 150 mM NaCl, 0.1% SDS, 1% Na deoxycholate, 1% NP-40), and incubated on ice for 20 min. The cells were then centrifuged at $12,000 \times g$ for 30 min at 4°C, and the supernatant was collected. The appropriate antibody was added to 400 μ l of lysate and incubated for 3 h at 4°C with rotation. Forty microliters of protein A-Sepharose beads was added, the mixture was incubated for 4 h at 4°C with rotation, and the resulting protein A-antibody complexes were washed five times with PBS. The immunoprecipitated proteins were then analyzed by SDS-PAGE, followed by Western blotting.

Alternative immunoprecipitation assay. The alternative immunoprecipitation assay was carried out as described by Chi and coworkers (4). Briefly, infected cells were harvested in 50 mM Tris-HCl (pH 7.6)–150 mM NaCl–0.5% NP-40–0.5 mM EDTA–2 mM dithiothreitol–protease inhibitors and incubated on ice for 30 min and then insoluble material was pelleted for 20 min at $13,000 \times g$ and 4°C. The resulting lysates were precleared with protein A-Sepharose beads for 20 min at 37°C and then incubated with fresh beads and the appropriate antibody for 15 min at 37°C. Following four washes with the lysis buffer, the bound material was analyzed by SDS-PAGE and Western blotting.

RESULTS

HSV-1 VP22 binds to VP16, gE, and gM but not gD in infected cells. HSV-1 VP22 has been reported to have a number of virus binding partners, namely, VP16, gE, and gD (4, 13, 19, 32, 33). In addition, PRV VP22 has been shown to interact with the cytoplasmic tail of gM (20). To further characterize the molecular interactions that HSV-1 VP22 exhibits during infection, we carried out coimmunoprecipitation assays with infected cells. Vero cells were infected with either the Δ 22 virus, expressing GFP in place of VP22, or the GFP-VP22-expressing virus at a multiplicity of 1 and harvested for immunoprecipitation 20 to 24 h after infection. Immunoprecipitation was carried out with a polyclonal anti-GFP antibody, and the resulting immunocomplexes were analyzed by SDS-PAGE, followed by Western blotting with a range of antibodies (Fig. 1A). GFP and GFP-22 were efficiently precipitated from the Δ 22- and GFP-22 infected cells, respectively, as demonstrated by blotting with a GFP monoclonal antibody. As shown previously (23), VP16 was efficiently coprecipitated with GFP-22 but not GFP. Likewise, gE was coprecipitated in a VP22-specific fashion. However, by contrast, there was no evidence for the presence of gD in the precipitated protein complex.

Interestingly, gM was also seen to coprecipitate with VP22 but the levels of gM in the Δ 22-infected cell extract were undetectable, making it unclear whether this binding was specific for VP22 (Fig. 1A, gM). As these samples had been boiled prior to analysis and gM is known to precipitate under these

conditions, we repeated the gM blot assay with samples that were heated to only 56°C before being loaded onto the gel. In this case, gM was detectable in both wild-type (WT)- and Δ 22-infected cell extracts but the levels in Δ 22 were somewhat lower (Fig. 1B, Input). While trace amounts of gM protein from the WT extract bound nonspecifically to beads in the absence of antibody (Fig. 1B, no Ab), the level present in the GFP-specific immunocomplexes was much greater (Fig. 1B, GFP IP), confirming that gM had coprecipitated with VP22. Furthermore, no gM was present in the immunoprecipitation from Δ 22-infected cells (Fig. 1B, GFP-IP), a result that was reproduced in a later experiment (see Fig. 8F), where the gM levels in the Δ 22-infected cell input extract were higher than in the experiment shown in Fig. 1. Taken together, these results suggest that HSV-1 gM interacts with HSV-1 VP22 in the infected cell.

The absence of gD after VP22 immunoprecipitation was an unexpected result, as it has been reported by other groups that these two proteins interact (4, 19). We repeated the experiment with antibodies specific to both the N and C termini of VP22 (AGV031 and AGV600, respectively) that are more efficient at immunoprecipitating than the GFP polyclonal antibody used above. However, no gD was detected in the pull-down complexes with these antibodies (data not shown). To determine if the inability to detect gD was due to the immunoprecipitation methodology used, we repeated the VP22 immunoprecipitation with antibody AGV031 from infected cells by the method from the previous study by Chi and coworkers (4). In addition, the reciprocal gD immunoprecipitation was carried out, followed by blotting for VP22. In both cases, although the target protein was efficiently precipitated, the putative partner protein was not detected (Fig. 1C). In a further attempt to demonstrate VP22 binding to gD, we next used a different method to detect VP22 binding proteins in infected cells. Full-length polyhistidine-tagged VP22 purified from baculovirus-infected sf9 cells was bound to nickel beads and incubated with an infected cell extract made from 2×10^8 Vero cells infected with strain 17 of HSV-1. Following 1 h of incubation at 4°C, the beads were washed extensively to remove nonbinding proteins and then the resulting VP22-specific complexes were eluted from the beads in 500- μ l fractions with 250 mM imidazole. These fractions were analyzed by SDS-PAGE, followed by Coomassie blue staining (Fig. 1D), indicating that at least one specific binding protein of around 65 kDa was detectable by staining. Western blotting of fractions 2 and 3 revealed that the major 65-kDa copurifying protein was VP16, while blotting for a second tegument protein, VP13/14, demonstrated that the VP16 binding to His-tagged VP22 was specific in nature. Importantly, blotting for gD showed no evidence of gD binding to VP22 in this assay. We conclude that in our experiments, although we demonstrated VP16, gE, and now gM interactions with VP22 during HSV-1 infection with ease, no gD interaction was detectable.

VP22 binds to VP16, gE, and gM in vitro. It has been shown previously that HSV-1 VP22 binds to the cytoplasmic tail of gE while PRV VP22 binds to the cytoplasmic tails of gE and gM (19, 20, 32). Therefore, to extend our observations on the VP22-interacting proteins described above, we first expressed and purified on glutathione-Sepharose beads the C-terminal 106 residues of gE, the C-terminal 126 residues of gM, and

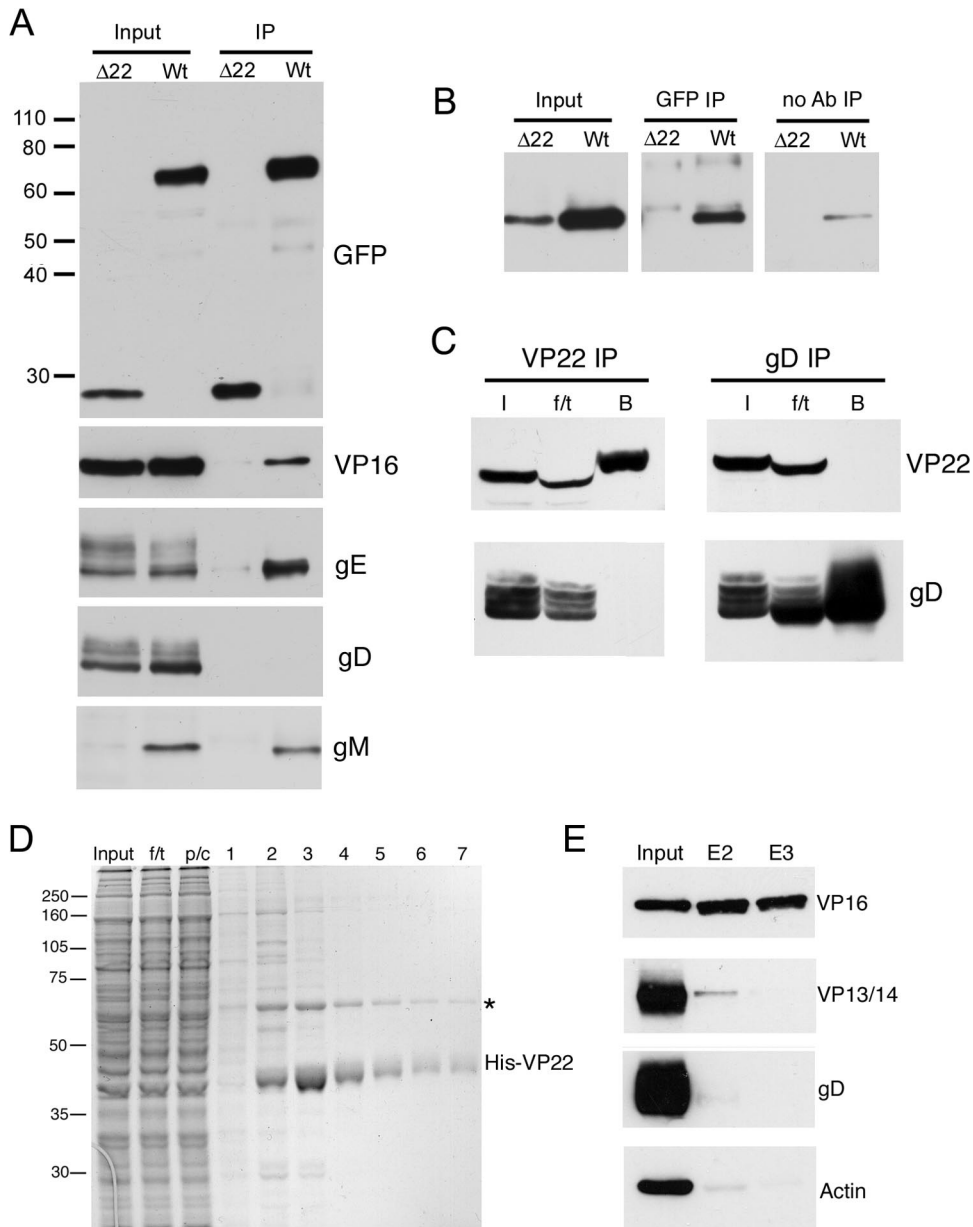


FIG. 1. Binding partners of VP22 in infected cells. (A) RIPA extracts were made from Vero cells infected with HSV-1 expressing GFP-VP22 (Wt) or HSV-1 expressing GFP in place of VP22 ($\Delta 22$), and immunoprecipitations were carried out with a polyclonal anti-GFP antibody. The resulting immunocomplexes (IP) were analyzed by SDS-PAGE, followed by Western blotting with antibodies for GFP, VP16, gE, gD, and gM. (B) Immunoprecipitations were carried out as for panel A, but samples in loading buffer were heated to 56°C rather than boiled before analysis by SDS-PAGE, followed by Western blotting for gM. A control immunoprecipitation in the absence of antibody was also carried out (no Ab). (C) Vero cells infected with strain 17 of HSV-1 were subjected to immunoprecipitation for VP22 and gD by the method of Chi and coworkers (4). I, input; f/t, flowthrough; B, bound. NB: the presence of the f/t sample on these gels has distorted the appearance of some bands. (D) Polyhistidine-tagged VP22 purified from baculovirus-infected Sf9 cells was bound to Ni-NTA beads and incubated for 1 h with a precleared cell extract from 10^8 strain 17-infected Vero cells. The beads were washed twice, and then bound material was eluted in 500- μ l aliquots. Samples were analyzed by SDS-PAGE, followed by Coomassie blue staining. f/t, flowthrough; p/c, precleared extract. The asterisk denotes the major 65-kDa VP22 binding protein. (E) Samples of the input extract and eluates 2 and 3 (E2 and E3) were analyzed by Western blotting with antibodies for VP16, VP13/14, gD, and actin. The values on the left are molecular sizes in kilodaltons.

full-length VP16 as GST fusion proteins. Equivalent amounts of these fusion proteins, together with unfused GST (Fig. 2A), were next used in pulldown assays in a manner similar to that described previously by O'Regan and coworkers (32). COS-1 cells were transfected with plasmids expressing GFP alone or

GFP-tagged VP22, and soluble extracts were prepared (Fig. 2B) and incubated with the GST fusion proteins bound to beads. After extensive washing, the protein complexes bound to the beads were solubilized and analyzed by SDS-PAGE, followed by Western blotting with an anti-GFP monoclonal

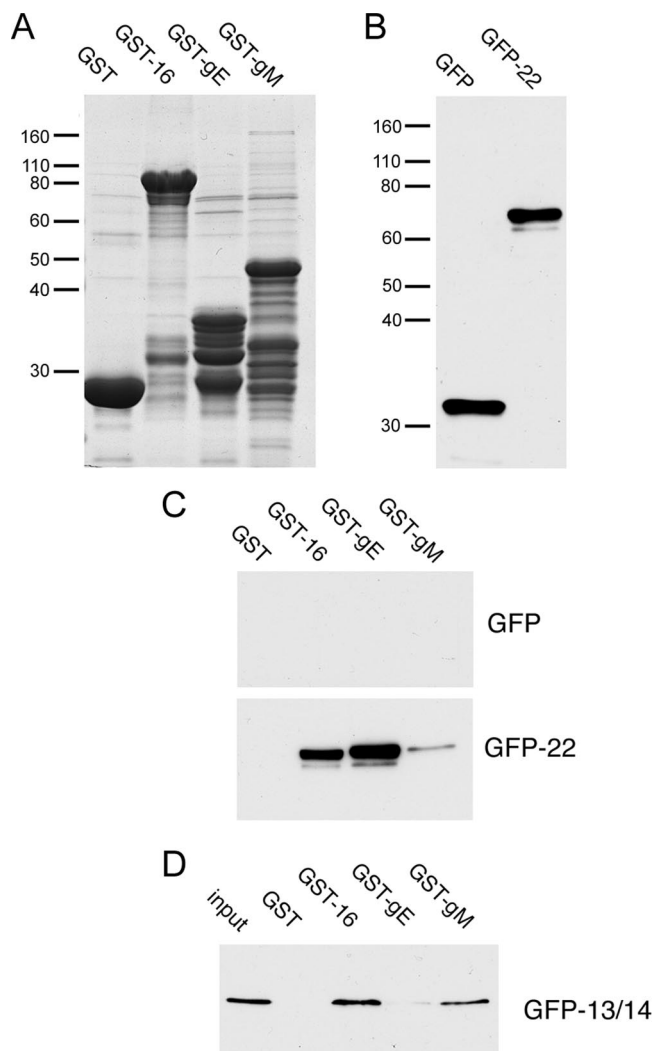


FIG. 2. In vitro binding of VP22 partners. (A) GST and GST fused to full-length VP16, the cytoplasmic tail of gE, or the cytoplasmic tail of gM were expressed and purified from *E. coli* strain BL21 and analyzed by SDS-PAGE, followed by Coomassie blue staining. (B) COS-1 cells were transfected with plasmids expressing GFP or GFP fused to full-length VP22, and soluble extracts were made and analyzed by SDS-PAGE, followed by Western blotting for GFP. (C) The extracts from panel B were incubated for 1 h with the GST fusion proteins shown in panel A that were already bound to glutathione-Sepharose beads. After extensive washing, the bound proteins were analyzed by SDS-PAGE, followed by Western blotting for GFP. (D) COS-1 cells were transfected with a plasmid expressing GFP fused to full-length VP13/14, and a soluble extract was made and analyzed for binding to the GST fusion proteins shown in panel A as described for panel C. The values on the left of panels A and B are molecular sizes in kilodaltons.

antibody. While GFP alone showed no binding activity to any of the fusion proteins, GFP-VP22 interacted efficiently with GST-gE and GST-VP16 but not GST alone (Fig. 2C), as described previously by others (32, 33). Interestingly, GFP-22 also bound, but more weakly, to the C-terminal tail of gM. To ensure that these results were not simply due to nonspecific stickiness of the glycoprotein tails, we used a GFP-tagged version of tegument protein VP13/14 in the same assay (Fig. 2D).

In this case, GFP-13/14 bound efficiently to GST-VP16, a result that confirms and extends our previous finding that VP13/14 interacts with VP16 in coimmunoprecipitation studies of infected cells (11). However, VP13/14 showed little binding to gE, indicating that the VP22 interaction with gE is specific. Moreover, VP13/14 bound efficiently to gM, hinting at an additional, as-yet-undescribed, tegument/envelope interaction.

The C terminus of VP22 contains a 93-residue gE binding domain. To investigate the region of VP22 involved in binding to these proteins, we expressed a range of GFP-tagged N- and C-terminal truncations of VP22 in COS-1 cells and tested them in our GST pull-down assays (Fig. 3A). The N-terminal 160 residues of VP22 showed no binding to GST-gE, while the C-terminal 140 residues bound as efficiently as the full-length protein, placing the gE binding domain in this C-terminal region of VP22 (Fig. 3B, compare GFP 1-160 with GFP 160-301). This is in agreement with the studies by O'Regan and coworkers (32). To refine the N-terminal limit of the gE binding domain, we then used a number of mutants with larger N-terminal truncations (Fig. 3A). Residues 174 to 301 bound to gE as efficiently as residues 160 to 301 (Fig. 3B, GFP 174-301), but a further truncation of 18 residues from the N terminus abolished the VP22-gE interaction (Fig. 3B, GFP 192-301). Hence, we can place the N-terminal limit of the gE binding domain of VP22 at residue 174 of the protein. The C-terminal limit of the gE binding domain was determined by using C-terminal truncation mutants expressing residues 1 to 212, 1 to 226, and 1 to 267, respectively. Of these three proteins, only the largest (residues 1 to 267) was able to bind to GST-gE in the pull-down assay (Fig. 3B), thereby placing the gE binding domain of VP22 within residues 174 to 267 of the protein.

gE recruits VP22 to the Golgi region of transfected cells. When VP22 is expressed in isolation by transient transfection, it localizes to cellular microtubules, which it reorganizes into characteristic bundles, a property that is maintained in the GFP-tagged variant (14, 15). By contrast, gE is reported to localize to the *trans*-Golgi network (TGN) in both virus infection and transient transfection (1, 27). Thus, we wished to determine the effect of coexpressing gE with VP22 on the localization of the two proteins. We first assessed the subcellular localization of gE in our assays by transfection of Vero cells, followed by immunofluorescence assays with both anti-gE and anti-TGN46 antibodies. As described by others (1), gE localized to a perinuclear site where it colocalized with the TGN marker TGN46 (Fig. 4, TGN, +gE). We next transfected Vero cells with full-length GFP-VP22 and a range of the truncated fusions described above either with or without gE. We have described the localization of these GFP-tagged mutant VP22 proteins in a previous paper (26). As we have previously shown, GFP-VP22 localized in a striking cytoplasmic filamentous pattern that is representative of reorganized microtubules (Fig. 4, 1-301, -gE). However, in the presence of gE, VP22 localization was dramatically altered to colocalization with gE in the Golgi region of the cell (Fig. 4, 1-301, +gE). Moreover, although the residue 174 to 301 mutant VP22 protein had lost the ability to reorganize microtubules (Fig. 4, 174-301, -gE), in the presence of gE this protein was also recruited to the Golgi region (Fig. 4, 174-301, +gE). By contrast, the 192 to 301 mutant VP22 protein exhibited the same cytoplasmic localization in the absence and presence of gE, indicating that these

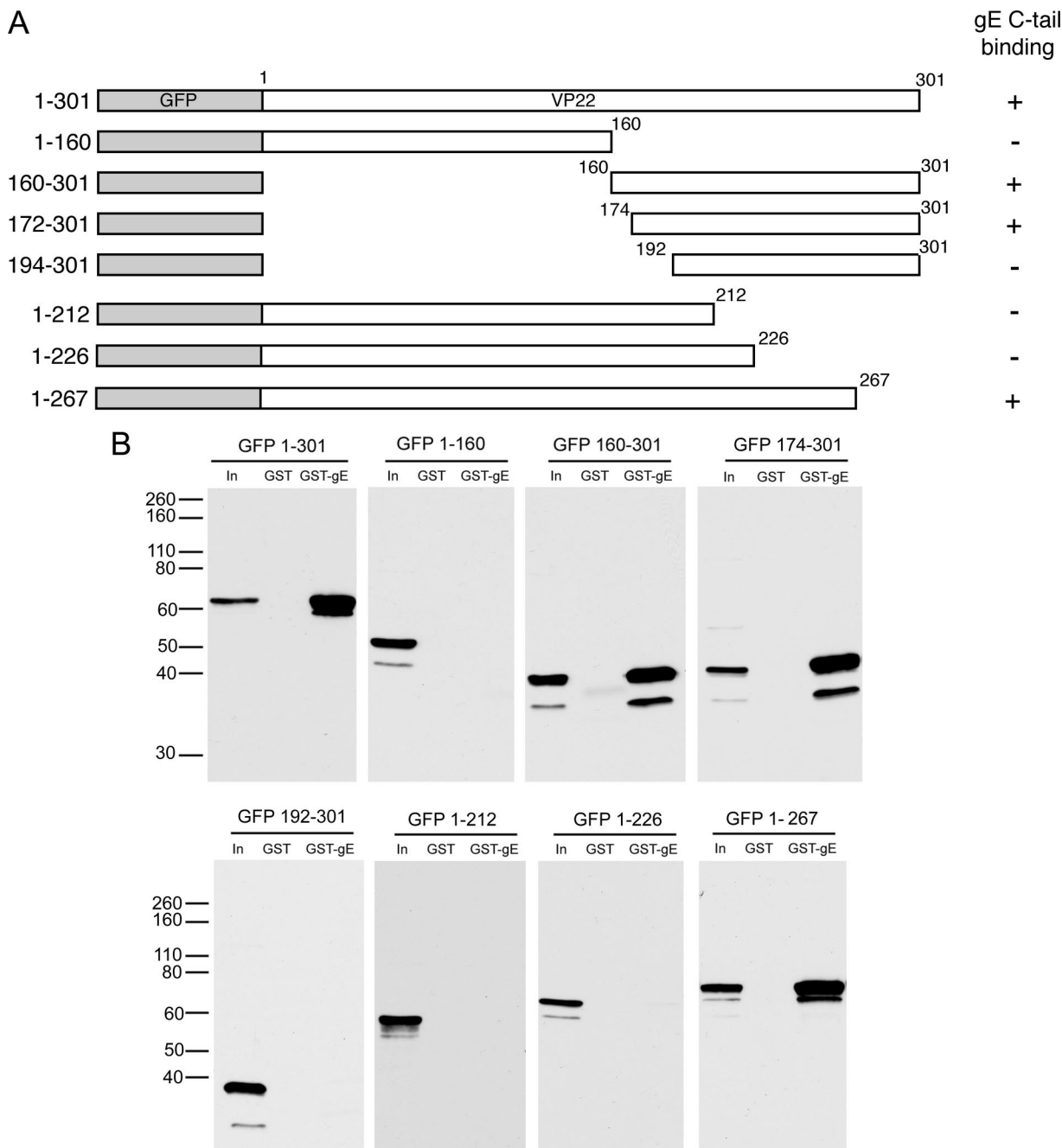


FIG. 3. gE binds to the packaging domain of VP22. (A) Line drawings of the N- and C-terminal truncation mutant forms of VP22 used in this study. (B) COS-1 cells were transfected with plasmids expressing each of the GFP-tagged mutant forms of VP22 shown in panel A, and soluble extracts were tested for the ability to bind GST or GST fused to the cytoplasmic tail of gE as described for Fig. 2C. The values on the left are molecular sizes in kilodaltons.

two proteins did not interact (Fig. 4, 192-301). These results are in agreement with the binding studies described above. Likewise, when the plasmids expressing the GFP-tagged C-terminal truncations expressing residues 1 to 212 and 1 to 267 of VP22 were cotransfected with gE, only the residue 1 to 267 variant was relocalized to the Golgi region of the cell (Fig. 4, compare 1-267 with 1-212). Hence, recruitment of the VP22 variants to the Golgi region by gE correlated directly with their ability to interact *in vitro*.

Characterization of the VP22-gM interaction. We next compared the nature of the VP22-gM interaction with that of the VP22-gE interaction by using GST pull-down assays of the VP22 truncation mutant proteins on the gM cytoplasmic tail. The results confirm that full-length VP22 is able to bind to the cytoplasmic tail of gM (Fig. 5A, 1-301). However, in contrast to gE, we were unable to define a minimal gM binding domain within VP22 that retained optimal binding, as every truncation mutant protein examined was greatly reduced in its ability to

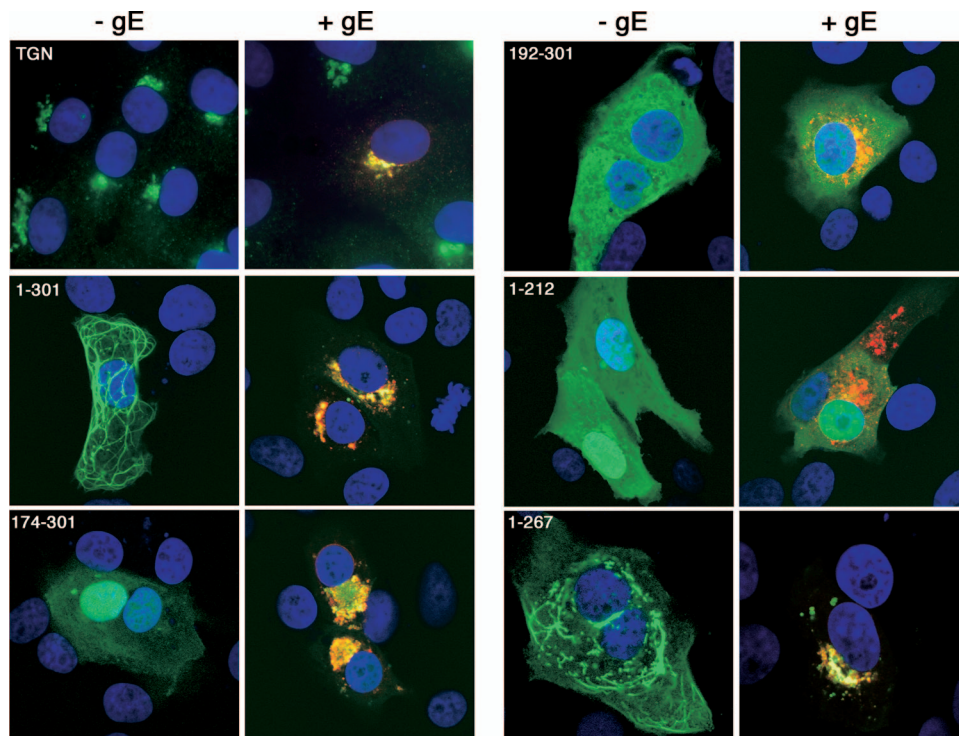


FIG. 4. gE recruits the packaging domain of VP22 to the secretory pathway. Vero cells grown on coverslips were transfected with plasmids expressing the denoted regions of VP22 as GFP fusion proteins (green) either in the absence or in the presence of a plasmid expressing gE. Twenty hours after transfection, cells were fixed with 4% paraformaldehyde and an immunofluorescence assay was carried out with the anti-gE antibody (red). Nuclei were stained with DAPI (blue). TGN denotes Vero cells processed for immunofluorescence with the anti-TGN 46 antibody.

bind gM (Fig. 5A and B). To determine if gM was able to recruit full-length VP22 to the secretory pathway in the same manner as gE, we next cotransfected Vero cells with plasmids expressing gM and GFP-VP22 and carried out immunofluorescence studies as described above. As expected, gM expressed alone localized to the Golgi/TGN region of the cell (Fig. 6A, gM alone). In contrast to coexpression of VP22 with gE, coexpression with gM had little effect on the microtubule pattern of VP22 and there was no evidence of colocalization of the two proteins (Fig. 6A, +1-301). While the gM pattern was relatively fragmented in the presence of VP22, we believe this is due to a general fragmentation of the secretory pathway induced by the VP22-specific microtubule reorganization. To confirm this, we expressed CFP-VP22 in Vero cells stably expressing a yellow fluorescent protein-Golgi body marker and showed extensive fragmentation of the Golgi body in comparison to that in untransfected cells (Fig. 6B). Finally, we expressed gM with a number of the truncation mutant VP22 proteins that retain reduced gM binding but saw no evidence of colocalization of these proteins that might indicate interaction (Fig. 6A, +1-212 and +160-301). Hence, we conclude that although we can demonstrate full-length VP22 binding to gM by using biochemical assays, this interaction is not reproduced in cotransfected cells in the same way as the gE interaction and that gM is unlikely to be an efficient direct binding partner of VP22 in the cellular environment.

A deletion of 14 residues from the gE binding domain abolishes VP22 interaction with gE. We next wished to construct a VP22 variant that was unable to bind gE by deleting as short a

region as possible in the 93-residue gE binding domain of full-length VP22. Three internal deletions were introduced into the construct expressing GFP-VP22—two within the gE binding domain ($\Delta 170-192$ and $\Delta 213-226$) and one just outside ($\Delta 160-172$) (Fig. 7A). These mutant proteins were tested in GST pulldown assays on the gE cytoplasmic tail as before, revealing that both mutations internal to the gE binding domain abolished gE binding (Fig. 7B). By contrast, the third mutation, which lies outside the gE binding domain, had no effect on the interaction, confirming that the results for the first two mutant proteins represent specific inhibition of the VP22-gE complex (Fig. 7B).

Mutation of the VP22 gE binding domain in HSV-1. We next addressed the role played by the VP22-gE interaction in virus infection by introducing the smallest mutation that we had identified to abolish gE binding by VP22, namely, $\Delta 213-226$ (now called $\Delta gEbind$). To construct a recombinant HSV-1 expressing VP22 $\Delta gEbind$ in place of WT VP22, we first constructed a transfer plasmid expressing this open reading frame as a GFP fusion protein, surrounded by its natural flanking sequences from the HSV-1 UL49 gene. This plasmid was cotransfected into Vero cells with infectious DNA from our previously described HSV-1 VP22 deletion mutant ($\Delta 22$) (12), and green fluorescent plaques were isolated and purified three times before characterization of the resulting virus. Consequently, we generated a virus expressing GFP-tagged VP22 ($\Delta gEbind$) that could be analyzed next to our viruses expressing GFP-tagged full-length VP22 (WT) (17) and GFP in place of VP22 ($\Delta 22$) (Fig. 8A). In the same way, we also constructed

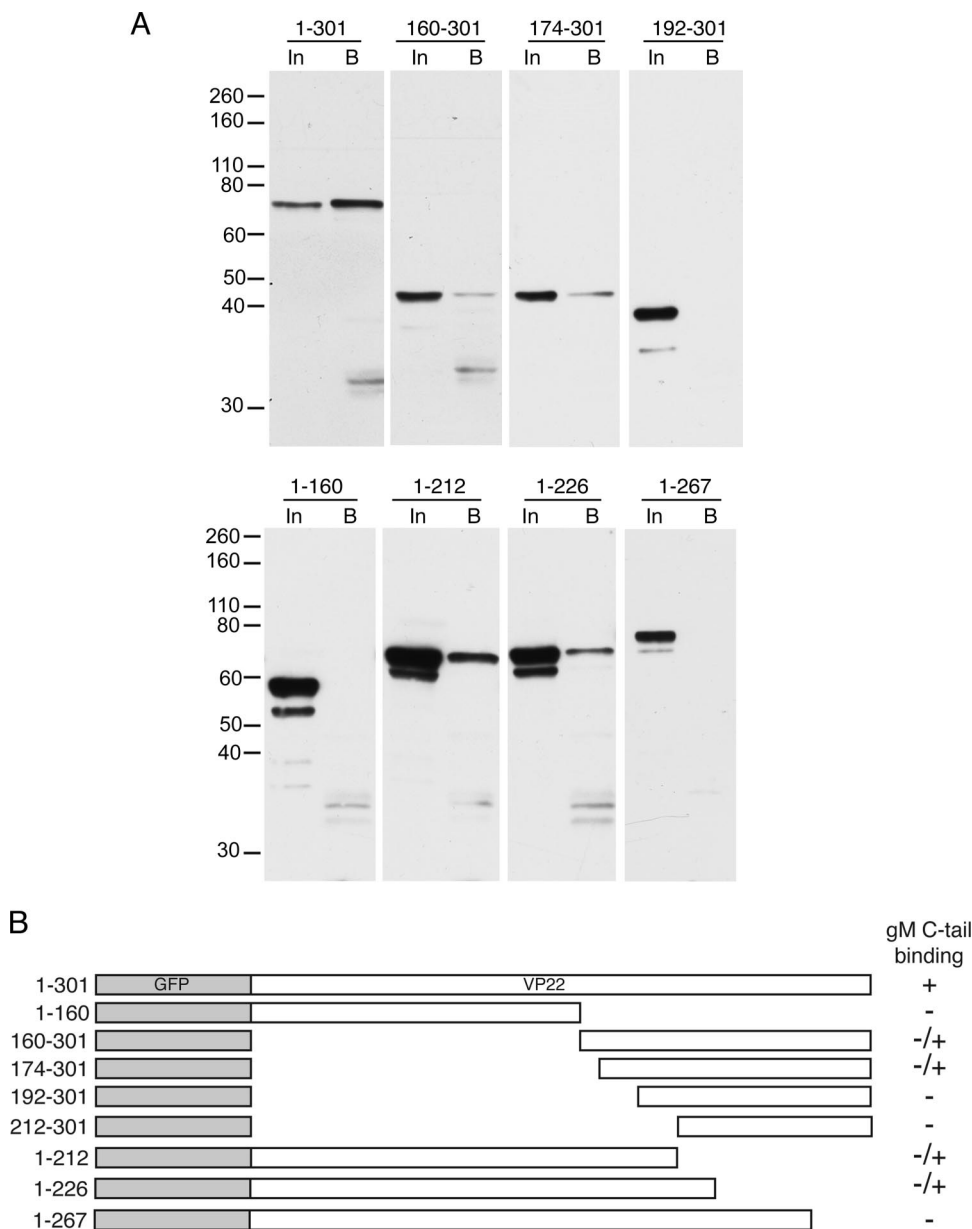


FIG. 5. gM binding to VP22. (A) COS-1 cells were transfected with plasmids expressing each of the GFP tagged mutant forms of VP22 shown in Fig. 3A, and soluble extracts were tested for the ability to bind GST fused to the cytoplasmic tail of gM as described for Fig. 2C. The values on the left are molecular sizes in kilodaltons. (B) Summary of the results shown in panel A. -/+ denotes binding that is greatly reduced compared to that of full-length VP22.

a second virus containing the $\Delta 170-192$ deletion described above, which was also shown to abolish the gE-VP22 interaction (Δ gEbind2 in Fig. 8A).

To assess the VP22 expression of the Δ gEbind virus, monolayers of Vero cells were infected at a multiplicity of 5 with recombinant HSV-1 expressing either full-length GFP-VP22 or GFP- Δ gEbind and harvested at various times after infection. Samples from each time point were then analyzed by Western blotting with a monoclonal anti-GFP antibody, which indicated that the GFP- Δ gEbind protein expressed during infection was the correct size and was expressed at the same time and to the same levels as full-length GFP-VP22 (Fig. 8B,

GFP). In addition, a blot for the tegument protein VP16 indicated that this second viral protein was also expressed at equivalent levels in both infections (Fig. 8B, VP16). We next used these viruses in the same GST pulldown assays that we had performed with transfected cell extracts. Vero cells were infected with viruses expressing either full-length GFP-VP22 (WT), mutant GFP-VP22 (Δ gEbind), or no VP22 ($\Delta 22$) and harvested 16 h after infection. Soluble extracts were incubated with GST-gE, GST-gM, or GST-VP16 bound to glutathione-Sepharose beads as before, and the resulting complexes were analyzed by SDS-PAGE, followed by Western blotting with the anti-GFP antibody (Fig. 8C). In this case, while the WT GFP-

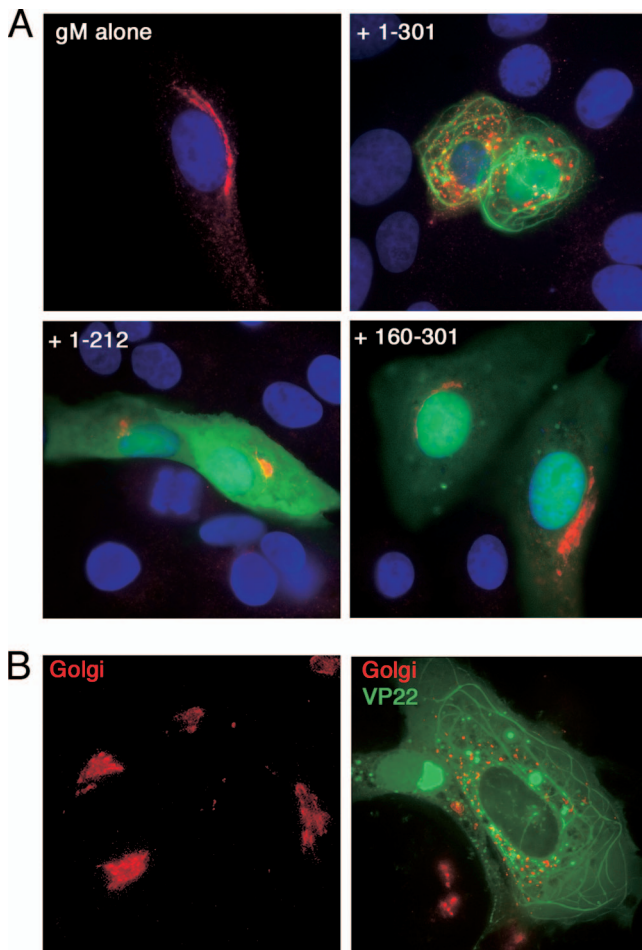


FIG. 6. gM does not alter the localization of VP22. (A) Vero cells grown on coverslips were transfected with plasmids expressing gM (red) and the denoted regions of VP22 as GFP fusion proteins (green). Twenty hours after transfection, cells were fixed with 4% paraformaldehyde and an immunofluorescence assay was carried out with the anti-gM antibody. Nuclei were stained with DAPI (blue). (B) A Vero cell line stably expressing a yellow fluorescent protein-tagged Golgi marker (red) was transfected with plasmid expressing GFP-tagged full-length VP22 (green) and examined by live cell fluorescence.

tagged VP22 protein bound efficiently to all three GST fusion proteins, the Δ gEbind protein bound only to GST-VP16.

To confirm that this mutant form of VP22 was unable to interact with gE within infected cells, extracts of infected cells were prepared in RIPA buffer and immunoprecipitations were carried out with a polyclonal anti-GFP antibody. The resulting purified complexes were analyzed by Western blotting with a monoclonal anti-GFP antibody to determine the efficiency of immunoprecipitation and with an antibody against gE to assess the VP22-gE interaction. Although the three GFP fusion proteins were precipitated by the GFP antibody with equal efficiency (Fig. 8D, GFP), only the full-length protein was able to coprecipitate gE (Fig. 8D, gE), confirming that the 14 residues between 213 and 226 of VP22 are required for gE binding in infection. Blotting of these immunoprecipitations for gD further confirmed that this glycoprotein does not interact with VP22 under these conditions. We next wished to determine if

the Δ gEbind mutant form of VP22 retained its ability to interact with VP16 in infected cells. In this case, VP22 was immunoprecipitated from infected cells with a polyclonal anti-VP22 antibody and the resulting complexes were blotted for GFP and VP16 to determine the level of VP16 that had coprecipitated with VP22. The full-length and Δ gEbind mutant proteins were both precipitated by the VP22 antibody with equal efficiency (Fig. 8E, VP22). In addition, VP16 also coimmunoprecipitated equally with both forms of VP22 but was not present in the sample immunoprecipitated from Δ 22-infected cells (Fig. 8E), confirming that the Δ gEbind mutant form of VP22 retains its ability to interact with its tegument protein partner, VP16, in infected cells.

In the process of these studies, we generated a second mutant virus expressing GFP-VP22 lacking residues 170 to 192 (Δ gEbind2 in Fig. 8A), which we had shown in our transfected cell assays to be unable to bind to the cytoplasmic tail of gE (Fig. 7B). Hence, we used this virus in coimmunoprecipitation assays with infected cells to provide further evidence that we had truly identified gE binding mutant proteins in our GST pulldown assays. VP22 was immunoprecipitated from infected cell extracts as before with a polyclonal anti-GFP antibody, and the resulting immunocomplexes were analyzed by Western blotting with an antibody against GFP, showing that all of the immunoprecipitations had worked efficiently (Fig. 8F, GFP). Western blotting with the gE antibody revealed that although all of the extracts contained high levels of gE, only full-length VP22 was able to coprecipitate the glycoprotein (Fig. 8F, gE), confirming that our second gE binding mutation virus (Δ gEbind2) was unable to interact with gE in the infected cell. Interestingly, blotting of these immunoprecipitations for gM showed that the Δ gEbind mutant form of VP22 was unable to complex with gM while the Δ gEbind2 mutant form appeared to coimmunoprecipitate a lower level of gM than the WT protein (Fig. 8F). By contrast, immunoprecipitations carried out with a VP22 polyclonal antibody and analyzed by Western blotting with a VP16 antibody indicated that all of the variants of VP22 were able to interact with VP16 (Fig. 8G, VP16).

The Δ gEbind mutant form of VP22 exhibits aberrant localization in infected cells. Vero cells infected with HSV-1 expressing GFP-tagged VP22 exhibit a characteristic fluorescence pattern at around 8 h postinfection in which VP22 localizes to numerous small complexes that are often clustered close to the nucleus (Fig. 9A, WT). We have previously provided evidence to suggest that localization of VP22 to these complexes correlates with efficient assembly of VP22 into the virus structure (23). Hence, to determine the effect of abolishing gE binding on VP22 localization to these complexes, we next determined the localization of GFP-VP22 Δ gEbind in Vero cells infected in the same manner and imaged 8 h after infection. Strikingly, GFP-VP22 lacking gE binding localized quite differently to WT GFP-VP22, with the mutant protein exhibiting a predominantly diffuse cytoplasmic localization (Fig. 9A, Δ gEbind). Unlike WT GFP-VP22, which eventually concentrates in the periphery of the infected cell at later times, the localization pattern of the mutant varied little as infection progressed (data not shown).

To assess the localization of VP22 in relation to gE in cells infected with these viruses, Vero cells at the same stage of infection were fixed and an immunofluorescence assay was

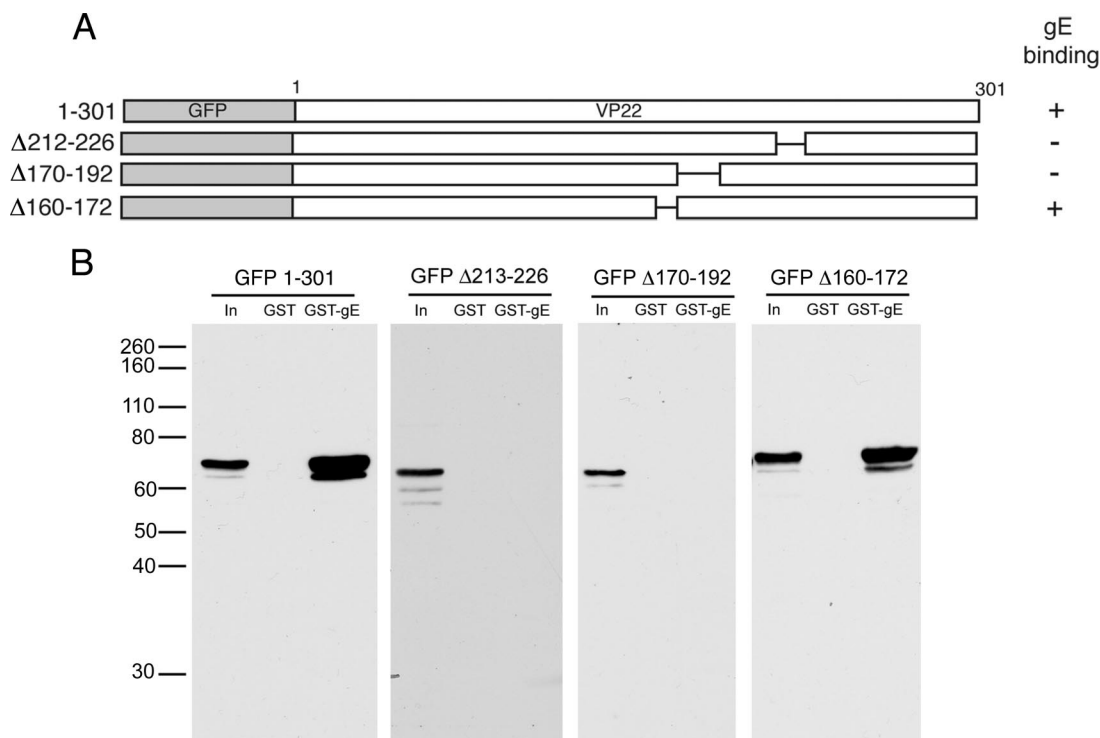


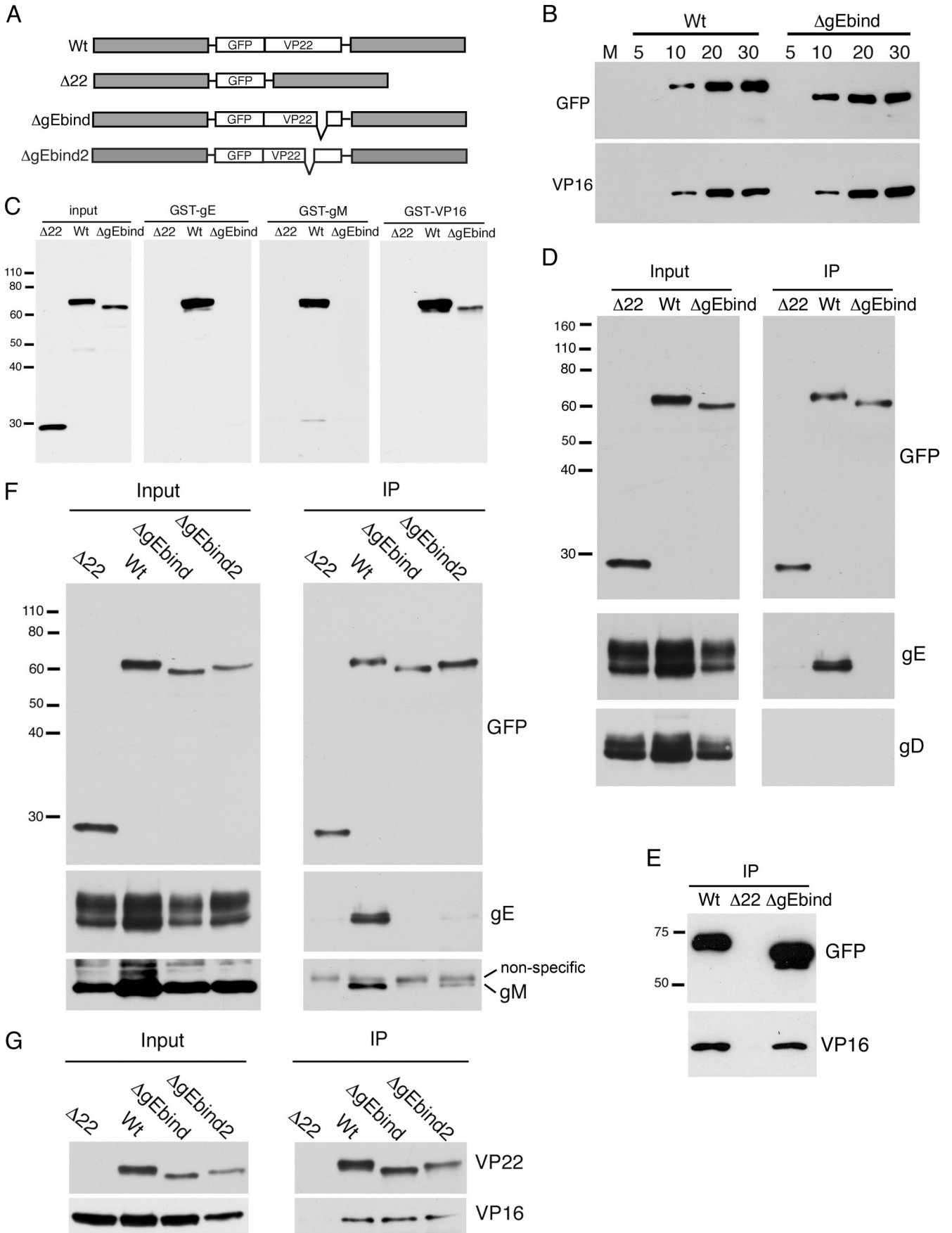
FIG. 7. Internal mutations within the gE binding domain of VP22 abrogate gE binding in vitro. (A) Line drawings of the three internal deletion mutant forms of VP22 constructed. (B) A plasmid expressing each of these mutants as GFP fusion proteins was transfected into COS-1 cells and analyzed for binding to GST and GST fused to the cytoplasmic tail of gE as described for Fig. 2C. The values on the left are molecular sizes in kilodaltons.

carried out with the anti-gE antibody. In WT-infected cells, it is clear that GFP-VP22 and gE are localized in large parts of the cell, particularly around the Golgi/TGN region (Fig. 9B, WT). By contrast, there is no overlap between GFP-VP22 and gE in the Δ gEbind-infected cells, correlating with the inability of this mutant to interact with gE (Fig. 9B, Δ gEbind). It is also noteworthy that although gE clearly localizes to the nuclear membrane of WT-infected cells, VP22 does not colocalize with gE at that site, suggesting that this population of gE is in some way different from that in the Golgi/TGN region.

Characterization of virions produced from virus expressing the Δ gEbind mutant form of VP22. We next wished to determine if the Δ gEbind mutant form of VP22 was capable of being assembled into virions. To determine if the incorporation of GFP-VP22 is affected by the gEbind mutation, we analyzed extracellular virions from viruses expressing full-length or Δ gEbind mutant VP22 by SDS-PAGE, followed by Coomassie blue staining, with equal amounts of the virion preparations loaded according to their major capsid protein (VP5) content. The stained virion profiles show that while full-length GFP-22 is discernible in these virions (Fig. 10A, arrowed band), no equivalent band of the correct size for the gEbind mutant protein was detected in virions produced by the mutant virus. To confirm that this protein is reduced in content in these virions, we next conducted Western blot assays with the same amount of each preparation. Blotting for VP5 showed that the virions were approximately equally loaded (Fig. 10B). However, blotting with antibodies against GFP clearly indicated that there were minimal levels of GFP-VP22

present in the Δ gEbind virions compared to that of the WT virions (Fig. 10B). Thus, deletion of only 14 residues from the VP22 open reading frame has a dramatic effect on both the localization and assembly of VP22 into the virus particle, suggesting that gEbind is a major determinant of VP22 recruitment to the virus. Furthermore, a similar reduction in VP22 content was observed in Δ gEbind2 virions (Fig. 10C). Finally, because we have shown previously that VP22 is required for the packaging of ICP0 into the virus tegument (12), we carried out Western blotting to detect the level of ICP0 present in the WT and Δ gEbind virions. Consistent with our previous results, this blot indicates that while ICP0 is easily detectable in WT virions, no ICP0 is present in Δ gEbind mutant virions, which package greatly reduced levels of VP22 (Fig. 10B, ICP0).

We have previously shown that HSV-1 lacking the VP22 open reading frame exhibits a cell-specific replication defect in epithelial MDBK cells (12). We have also shown that this defect can be rescued by both WT VP22 and a variant of VP22 in which all of the phosphorylation sites have been mutated (12, 36). Therefore, we next wished to determine if introduction of the gEbind mutant form of VP22 into the Δ 22 virus was also capable of rescuing this replication defect. Monolayers of confluent MDBK cells were infected at a low multiplicity with HSV-1 expressing either the full-length or the Δ gEbind mutant protein or with virus lacking the VP22 gene (Δ 22), and total virus was harvested at a range of times after infection. The resulting samples were titrated on Vero cells to determine the efficiency of virus replication in MDBK cells (Fig. 10D). In agreement with our previous results, there was a clear replica-



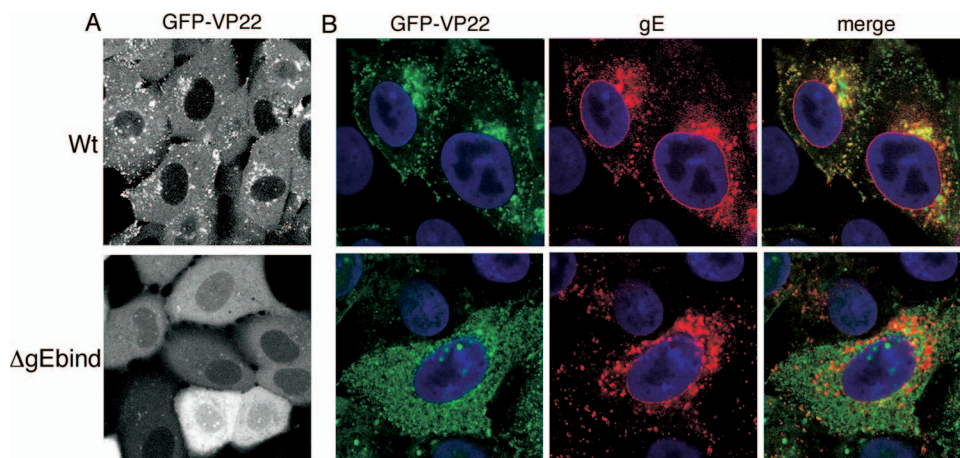


FIG. 9. VP22 colocalization with gE in infected cells is specific to its gE interaction domain. (A) Vero cells were infected with HSV-1 expressing GFP-22 or GFP- Δ gEbind at a multiplicity of 5 and examined live by fluorescence microscopy 8 h after infection. (B) Vero cells were infected with HSV-1 expressing GFP-22 or GFP- Δ gEbind at a multiplicity of 5 and fixed with 4% paraformaldehyde 8 h after infection. An immunofluorescence assay was carried out with the anti-gE antibody (red), and nuclei were stained with DAPI (blue).

tion defect of the Δ 22 virus compared to the WT virus in this experiment. Interestingly, the virus expressing the Δ gEbind mutant form of VP22 also replicated poorly in MDBK cells compared to the WT virus, a result that was highly reproducible (Fig. 10E). Taken together, these results suggest that a deletion of only 14 residues from the VP22 open reading frame is sufficient to mimic a complete deletion of the gene in virus replication in MDBK cells.

DISCUSSION

A major aim in the field of herpesvirus assembly is to understand the molecular mechanisms involved in recruiting the large number of virus-encoded proteins that end up in the tegument of the virus particle. Several potential recruitment strategies could be used in the process of virus tegumentation, including passive acquisition of proteins that happen to be in the vicinity of the assembly site, targeting by interaction with specific cellular proteins, or recruitment to assembling particles by protein-protein interactions with other virus proteins. In recent years, there have been a number of reports that support the latter strategy as the mechanism for tegument protein packaging (see below), but no single protein-protein

interaction has been proven to be required for a tegument protein to be packaged.

The molecular events involved in tegumentation have been previously investigated by using a range of techniques to search for relevant protein-protein interactions. For example, the PRV UL36 protein has been shown to interact with an outer capsid protein, UL25, providing evidence for a position for UL36 close to the capsid (5). Yeast two-hybrid studies have revealed a list of potential tegument-tegument interactions that may be involved in the recruitment of the other tegument proteins, although the significance of many of these has not yet been explored in the context of virus infection (42). In addition, pulldown experiments with the cytoplasmic tails of a number of HSV-1 glycoproteins have shown interactions between tegument proteins and envelope proteins such as VP16-gH, VP22-gD, VP22-gE, UL11-gD, and UL11-gE (4, 19, 22, 32). Nonetheless, none of these interactions has been shown to be crucial for tegument protein recruitment and it has been suggested that redundancy may exist among tegument/envelope interactions.

Our aim in the present study was to dissect the molecular interaction(s) involved in the recruitment of HSV-1 VP22 into the virus particle. VP22 is not absolutely essential for HSV-1

FIG. 8. Small mutations within the gE binding domain of VP22 inhibit the VP22-gE interaction in infected cells. (A) Line drawings of the viruses used in this study. Δ gEbind and Δ gEbind2 represent the Δ 213-226 and Δ 170-192 mutations shown in Fig. 7, respectively. (B) Vero cells were infected with HSV-1 expressing WT GFP-VP22 or GFP-VP22 (Δ gEbind) at a multiplicity of 2, and total extracts were obtained at various times after infection. These samples were analyzed by SDS-PAGE, followed by Western blotting with antibodies against GFP and VP16. (C) Soluble extracts were made from Vero cells infected with the Δ 22, WT, or Δ gEbind virus and used in binding assays with GST fused to the cytoplasmic tail of gE, the cytoplasmic tail of gM, or full-length VP16 as described for Fig. 2C. (D) Immunoprecipitations were carried out with the polyclonal GFP antibody on RIPA extracts of cells infected with the Δ 22, WT, or Δ gEbind virus, and the resulting immunocomplexes were analyzed by Western blotting with antibodies against GFP, gE, and gD. (E) Immunoprecipitations were carried out as for panel D but with the polyclonal anti-VP22 antibody AGV031. The resulting immunocomplexes were analyzed by Western blotting with antibodies against GFP and VP16. (F) Immunoprecipitations were carried out with the polyclonal GFP antibody on RIPA extracts of cells infected with the Δ 22, WT, Δ gEbind, or Δ gEbind2 virus, and the resulting immunocomplexes were analyzed by Western blotting with antibodies against GFP, gE, and gM. Nonspecific refers to cross-reacting species that appeared in all pulldown lanes with a molecular weight higher than that of gM. (G) Immunoprecipitation assays were carried out as for panel F but with the polyclonal anti-VP22 antibody AGV031. The resulting immunocomplexes were analyzed by Western blotting with antibodies against GFP and VP16. The values on the left of panels C to F are molecular sizes in kilodaltons.

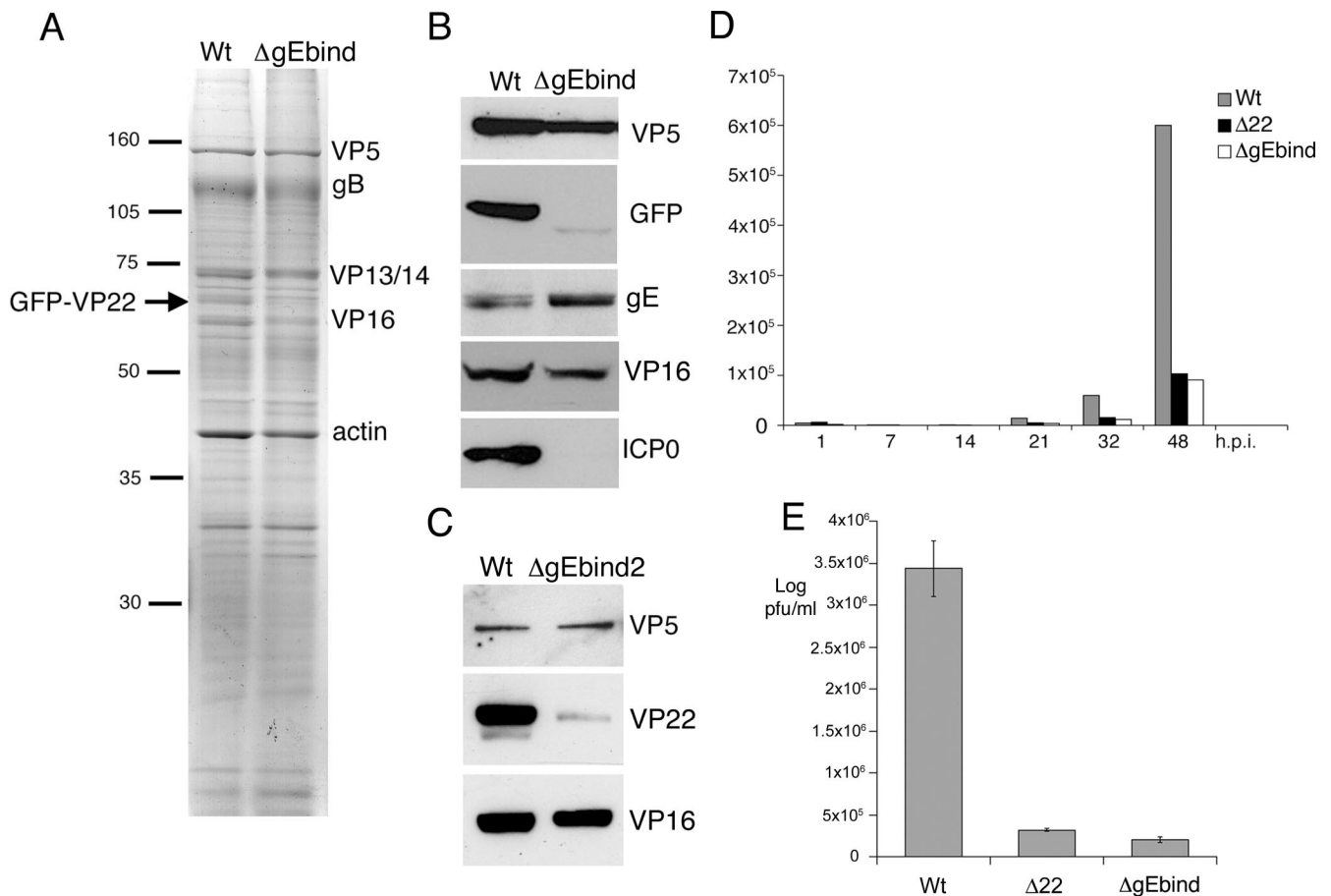


FIG. 10. VP22 is recruited to the HSV-1 virion by its interaction with gE. (A) Extracellular virions were purified from BHK cells infected with HSV-1 expressing GFP-VP22 or GFP- Δ gEbind and analyzed by SDS-PAGE, followed by Coomassie blue staining. (B) The same extracellular virions shown in panel A were analyzed by Western blotting with antibodies against the major capsid protein VP5, GFP, gE, VP16, and ICP0. (C) Extracellular virions were purified from BHK cells infected with HSV-1 expressing GFP-VP22 or GFP- Δ gEbind2 and analyzed by SDS-PAGE, followed by Western blotting with antibodies against the major capsid protein VP5, VP22, and VP16. (D) MDBK cells were infected with the Δ 22, WT, or Δ gEbind virus at a multiplicity of 0.1, and total samples were taken up to 48 h after infection. Samples were titrated on Vero cells. (E) MDBK cells were infected as for panel D, but samples were taken only at 48 h after infection. This experiment was carried out in triplicate. The values on the left of panel A are molecular sizes in kilodaltons.

growth in cell culture (12), and hence it is possible to introduce mutations into the protein and determine the effect on levels packaged into the tegument. In this way, we have previously shown that while the N-terminal half of the protein is dispensable for VP22 assembly, the C-terminal half is absolutely required, suggesting that the C terminus contains a virus packaging signal (23). This region of VP22 has been shown to contain both a VP16 and a gE binding domain (23, 32, 33). Our starting position was to revisit the population of VP22 binding proteins present in the infected cell by using coimmunoprecipitation assays, whereby we demonstrated VP16 and gE interaction with ease. Furthermore, in line with data from PRV, we also showed an interaction between VP22 and gM that had not yet been characterized in HSV-1 infection (20). However, unlike two other groups, we were unable to demonstrate an interaction with gD by using three different methods, and therefore we suggest that if the VP22-gD interaction exists, it is by nature extremely weak compared to the interactions with VP16, gE, and gM.

According to our GST-gE pulldown assays, the gE binding

domain is present within residues 174 to 267 of VP22, confirming and refining the previously defined gE binding domain of VP22 (32). Interestingly, coexpression of gE with the C-terminal half of VP22 by transient transfection resulted in gE recruiting VP22 to the Golgi region of the cell, suggesting that gE is sufficient to recruit VP22 to cellular membranes. This relocalization occurs even in the case of full-length VP22, which localizes to microtubules when expressed in isolation, implying that gE is the dominant partner in this relationship. Taken together, these results show that the C-terminal packaging domain of VP22 is sufficient for gE interaction and recruitment to the secretory pathway. We were able to abrogate the VP22-gE interaction by introducing a small 14-residue deletion into the gE binding domain and subsequently introduced this small mutation into the virus to address the role of gE binding in VP22 packaging into the virus. Characterization of this and a second virus with a different mutation in this region showed that gE binding correlated with the localization of VP22 within the cell and its recruitment to the virus tegument. Taken together, these results explain our previous data

on viruses expressing truncation mutant forms of VP22, where we showed that any mutant expressing a shorter C-terminal region than 160 to 301 was unable to localize to trafficking complexes or assemble efficiently into the virus (23). At that time, we interpreted this as a dependence on VP16, as the binding domain for VP16 is also present in the C-terminal half of VP22. However, it is clear from our present studies that none of the viruses we used in that study would have separated VP16 binding from gE binding. By contrast, the two gE binding mutant proteins we have constructed in this study are still able to interact with VP16 and yet are not packaged into the virus, suggesting that gE binding is absolutely required. While we cannot rule out an additional requirement for VP16 binding in VP22 assembly from our own studies, as we do not yet have a virus expressing a VP22 variant that binds gE but not VP16, O'Regan and coworkers have concluded that VP16 is not required for VP22 assembly into the virion (33).

Our coimmunoprecipitation studies with infected cells implicated gM as another potential partner in VP22 recruitment to the virus. However, it is possible that the gM present in these VP22-specific immunocomplexes does not interact directly with VP22 but precipitates with a VP22 binding partner. In support of this, although we could demonstrate an interaction between full-length VP22 and the cytoplasmic tail of gM in our pulldown assays, this interaction did not map to the VP22 packaging domain but seemed to require the full-length protein for optimal interaction. Furthermore, this interaction did not result in a relocalization of either protein in cotransfected cells. In addition, in cells infected with our second mutant virus, Δ gEbind2, VP22 was able to at least partially interact with gM in coimmunoprecipitations while not being recruited to the virion. Hence, we conclude that the VP22-gM interaction is unlikely to have a role in VP22 packaging.

Although the tegument was originally described as an amorphous layer, it now seems as if it may be a more ordered structure and that tegument proteins may be added sequentially to the capsid as it progresses through its maturation pathway (29). Furthermore, tegument proteins have been divided into inner and outer components by some workers, according to the ease with which they can be biochemically removed from the purified virus particle, with the assumption that inner components (the hardest to extract) would be the first to be recruited during assembly while the outer components would be the last to be added in the maturation pathway (43). Morphogenesis studies with viruses lacking individual essential tegument proteins have also been used to define the order of tegument protein incorporation, depending on the stage at which virus morphogenesis is blocked. For example, in the case of PRV and HSV-1 UL36 and UL37 gene mutants, morphogenesis has been shown to be blocked at early stages in the cytoplasm, thereby defining these two proteins as the innermost tegument proteins (8, 9, 21, 25). Our results obtained with cotransfected and infected cells suggest that gE recruits VP22 to the cytoplasmic face of membranes within the Golgi region of the cell. Because gE has been previously characterized to reside in the TGN in both infected cells and transfected cells, we therefore suggest that gE recruits VP22 to the cytoplasmic side of the TGN. This is in agreement with previous studies that indicate the TGN and/or endosomal membranes as the site of final virus envelopment (10, 24, 41). Nonetheless,

because the Golgi and TGN compartments are closely associated in the cell, it is difficult to differentiate between them by using cell markers in immunofluorescence alone, and further studies are required to determine if VP22 first associates with gE in the Golgi body or in the TGN.

One question that remains to be answered is whether the population of VP22 that is recruited by gE is already part of the assembling capsid at the time that it encounters the cytoplasmic tail of gE. The fact that the two proteins are seen to colocalize as early as 6 h after infection might suggest that the VP22-gE interaction occurs before the majority of capsids have entered the maturation pathway. Furthermore, it has recently been shown that the inner tegument protein UL37 localizes to the Golgi region of the cell in the absence of capsid structures but in a UL36-specific fashion, implying that even the innermost proteins in the tegument may be targeted to the envelopment site without prior association with capsids (7). It is also of note that although gE is present within the nuclear membrane, as well as the Golgi region, VP22 is not recruited to the nuclear rim during infection, suggesting that the two populations of gE may differ. Interestingly, only the faster migrating species of gE present in the infected cell appeared to coimmunoprecipitate with VP22 (Fig. 1A), suggesting that VP22 can discriminate between different forms of gE due to, for example, differential glycosylation or phosphorylation of gE (30, 34).

The growth phenotype of our Δ gEbind mutant virus that lacks only 14 amino acids of VP22 is equivalent to that of our VP22 knockout virus (12), whereby both viruses produce small plaques and show a replication defect in epithelial cells. This suggests that the phenotype of the VP22 knockout virus is primarily due to the absence of VP22 in the infecting virion rather than the lack of VP22 expression throughout infection. As both mutant viruses also fail to package the immediate-early protein ICP0, which we have shown to be assembled in a VP22-dependent fashion, it is possible that the phenotype may be explained in part by the absence of ICP0 in the incoming virions. Interestingly, the phenotype of an HSV-1 gE knockout virus is also poor spreading in epithelial cells (2, 10) and as our results predict that a Δ gE mutant virus would not package VP22 or ICP0, the Δ gE mutant virus phenotype may also be related in part to the absence of VP22 and/or ICP0 from the virion. Finally, it is of note that, in the cases of Marek's disease virus and varicella zoster virus, both gE and VP22 are absolutely essential for virus spreading (31, 39). Unlike HSV-1 or PRV, these viruses do not release free virus but remain cell associated and are entirely dependent on direct cell-to-cell spreading to infect neighboring cells. Hence, the phenotypes that we observe for gE and VP22 mutants of HSV-1 represent the less extreme end of the spectrum of requirement for gE-VP22 activities in alphaherpesvirus infection and may help define a unifying role for these proteins across the alphaherpesviruses.

ACKNOWLEDGMENTS

We thank Colin Crump for the constructs expressing GST-gE and GST-gM and the human CMV expression vector for gM. We also thank Helena Browne for the gM antibody and the gE expression vector, Peter O'Hare for the GST-VP16-expressing construct, David Johnson for the gE antibody, and Roger Everett for the ICP0 antibody.

This work was funded by the Medical Research Council and Marie Curie Cancer Care.

REFERENCES

1. Alconada, A., U. Bauer, B. Sodeik, and B. Hofflack. 1999. Intracellular traffic of herpes simplex virus glycoprotein gE: characterization of the sorting signals required for its *trans*-Golgi network localization. *J. Virol.* **73**:377–387.
2. Balan, P., N. Davis-Poynter, S. Bell, H. Atkinson, H. Browne, and T. Minson. 1994. An analysis of the *in vitro* and *in vivo* phenotypes of mutants of herpes simplex virus type 1 lacking glycoproteins gG, gE, gI or the putative gJ. *J. Gen. Virol.* **75**(Pt. 6):1245–1258.
3. Brunetti, C. R., K. S. Dingwell, C. Wale, F. L. Graham, and D. C. Johnson. 1998. Herpes simplex virus gD and virions accumulate in endosomes by mannose 6-phosphate-dependent and -independent mechanisms. *J. Virol.* **72**:3330–3339.
4. Chi, J. H., C. A. Harley, A. Mukhopadhyay, and D. W. Wilson. 2005. The cytoplasmic tail of herpes simplex virus envelope glycoprotein D binds to the tegument protein VP22 and to capsids. *J. Gen. Virol.* **86**:253–261.
5. Coller, K. E., J. I. Lee, A. Ueda, and G. A. Smith. 2007. The capsid and tegument of the alphaherpesviruses are linked by an interaction between the UL25 and VP1/2 proteins. *J. Virol.* **81**:11790–11797.
6. Dargin, D. 1986. The structure and assembly of herpes viruses, p. 359–437. *In* J. R. Harris and R. W. Horne (ed.), *Electron microscopy of proteins*, vol. 5. Academic Press, London, United Kingdom.
7. Desai, P., G. L. Sexton, E. Huang, and S. Person. 2008. Localization of herpes simplex virus type 1 UL37 in the Golgi complex requires UL36 but not capsid structures. *J. Virol.* **82**:11354–11361.
8. Desai, P., G. L. Sexton, J. M. McCaffery, and S. Person. 2001. A null mutation in the gene encoding the herpes simplex virus type 1 UL37 polypeptide abrogates virus maturation. *J. Virol.* **75**:10259–10271.
9. Desai, P. J. 2000. A null mutation in the UL36 gene of herpes simplex virus type 1 results in accumulation of unenveloped DNA-filled capsids in the cytoplasm of infected cells. *J. Virol.* **74**:11608–11618.
10. Dingwell, K. S., C. R. Brunetti, R. L. Hendricks, Q. Tang, M. Tang, A. J. Rainbow, and D. C. Johnson. 1994. Herpes simplex virus glycoproteins E and I facilitate cell-to-cell spread *in vivo* and across junctions of cultured cells. *J. Virol.* **68**:834–845.
11. Donnelly, M., J. Verhagen, and G. Elliott. 2007. RNA binding by the herpes simplex virus type 1 nucleocytoplasmic shuttling protein UL47 is mediated by an N-terminal arginine-rich domain that also functions as its nuclear localization signal. *J. Virol.* **81**:2283–2296.
12. Elliott, G., W. Hafezi, A. Whiteley, and E. Bernard. 2005. Deletion of the herpes simplex virus VP22-encoding gene (UL49) alters the expression, localization, and virion incorporation of ICP0. *J. Virol.* **79**:9735–9745.
13. Elliott, G., G. Mouzakis, and P. O'Hare. 1995. VP16 interacts via its activation domain with VP22, a tegument protein of herpes simplex virus, and is relocated to a novel macromolecular assembly in coexpressing cells. *J. Virol.* **69**:7932–7941.
14. Elliott, G., and P. O'Hare. 2000. Cytoplasm-to-nucleus translocation of a herpesvirus tegument protein during cell division. *J. Virol.* **74**:2131–2141.
15. Elliott, G., and P. O'Hare. 1998. Herpes simplex virus type 1 tegument protein VP22 induces the stabilization and hyperacetylation of microtubules. *J. Virol.* **72**:6448–6455.
16. Elliott, G., and P. O'Hare. 1997. Intercellular trafficking and protein delivery by a herpesvirus structural protein. *Cell* **88**:223–233.
17. Elliott, G., and P. O'Hare. 1999. Live-cell analysis of a green fluorescent protein-tagged herpes simplex virus infection. *J. Virol.* **73**:4110–4119.
18. Elliott, G. D., and D. M. Meredith. 1992. The herpes simplex virus type 1 tegument protein VP22 is encoded by gene UL49. *J. Gen. Virol.* **73**(Pt. 3):723–726.
19. Farnsworth, A., T. W. Wisner, and D. C. Johnson. 2007. Cytoplasmic residues of herpes simplex virus glycoprotein gE required for secondary envelopment and binding of tegument proteins VP22 and UL11 to gE and gD. *J. Virol.* **81**:319–331.
20. Fuchs, W., B. G. Klupp, H. Granzow, C. Hengartner, A. Brack, A. Mundt, L. W. Enquist, and T. C. Mettenleiter. 2002. Physical interaction between envelope glycoproteins E and M of pseudorabies virus and the major tegument protein UL49. *J. Virol.* **76**:8208–8217.
21. Fuchs, W., B. G. Klupp, H. Granzow, and T. C. Mettenleiter. 2004. Essential function of the pseudorabies virus UL36 gene product is independent of its interaction with the UL37 protein. *J. Virol.* **78**:11879–11889.
22. Gross, S. T., C. A. Harley, and D. W. Wilson. 2003. The cytoplasmic tail of herpes simplex virus glycoprotein H binds to the tegument protein VP16 *in vitro* and *in vivo*. *Virology* **317**:1–12.
23. Hafezi, W., E. Bernard, R. Cook, and G. Elliott. 2005. Herpes simplex virus tegument protein VP22 contains an internal VP16 interaction domain and a C-terminal domain that are both required for VP22 assembly into the virus particle. *J. Virol.* **79**:13082–13093.
24. Harley, C. A., A. Dasgupta, and D. W. Wilson. 2001. Characterization of herpes simplex virus-containing organelles by subcellular fractionation: role for organelle acidification in assembly of infectious particles. *J. Virol.* **75**:1236–1251.
25. Klupp, B. G., H. Granzow, E. Mundt, and T. C. Mettenleiter. 2001. Pseudorabies virus UL37 gene product is involved in secondary envelopment. *J. Virol.* **75**:8927–8936.
26. Martin, A., P. O'Hare, J. McLauchlan, and G. Elliott. 2002. The herpes simplex virus tegument protein VP22 contains overlapping domains for cytoplasmic localization, microtubule interaction, and chromatin binding. *J. Virol.* **76**:4961–4970.
27. McMillan, T. N., and D. C. Johnson. 2001. Cytoplasmic domain of herpes simplex virus gE causes accumulation in the *trans*-Golgi network, a site of virus envelopment and sorting of virions to cell junctions. *J. Virol.* **75**:1928–1940.
28. Mettenleiter, T. C. 2002. Herpesvirus assembly and egress. *J. Virol.* **76**:1537–1547.
29. Mettenleiter, T. C. 2006. Intriguing interplay between viral proteins during herpesvirus assembly or: the herpesvirus assembly puzzle. *Vet. Microbiol.* **113**:163–169.
30. Miriagou, V., L. Stevanato, R. Manservigi, and P. Mavromara. 2000. The C-terminal cytoplasmic tail of herpes simplex virus type 1 gE protein is phosphorylated *in vivo* and *in vitro* by cellular enzymes in the absence of other viral proteins. *J. Gen. Virol.* **81**:1027–1031.
31. Moffat, J., C. Mo, J. J. Cheng, M. Sommer, L. Zerbini, S. Stamatis, and A. M. Arvin. 2004. Functions of the C-terminal domain of varicella-zoster virus glycoprotein E in viral replication *in vitro* and skin and T-cell tropism *in vivo*. *J. Virol.* **78**:12406–12415.
32. O'Regan, K. J., M. A. Bucks, M. A. Murphy, J. W. Wills, and R. J. Courtney. 2007. A conserved region of the herpes simplex virus type 1 tegument protein VP22 facilitates interaction with the cytoplasmic tail of glycoprotein E (gE). *Virology* **358**:192–200.
33. O'Regan, K. J., M. A. Murphy, M. A. Bucks, J. W. Wills, and R. J. Courtney. 2007. Incorporation of the herpes simplex virus type 1 tegument protein VP22 into the virus particle is independent of interaction with VP16. *Virology* **369**:263–280.
34. Para, M. F., R. B. Baucke, and P. G. Spear. 1982. Glycoprotein gE of herpes simplex virus type 1: effects of anti-gE on virion infectivity and on virus-induced Fc-binding receptors. *J. Virol.* **41**:129–136.
35. Phelan, A., G. Elliott, and P. O'Hare. 1998. Intercellular delivery of functional p53 by the herpesvirus protein VP22. *Nat. Biotechnol.* **16**:440–443.
36. Potel, C., and G. Elliott. 2005. Phosphorylation of the herpes simplex virus tegument protein VP22 has no effect on incorporation of VP22 into the virus but is involved in optimal expression and virion packaging of ICP0. *J. Virol.* **79**:14057–14068.
37. Rixon, F. 1993. Structure and assembly of herpesviruses. *Semin. Virol.* **4**:135–144.
38. Roizman, B., and A. E. Sears. 1991. Herpes simplex viruses and their replication, p. 849–895. *In* B. N. Fields and D. M. Knipe (ed.), *Fundamental virology*, 2nd ed. Raven Press, New York, NY.
39. Schumacher, D., B. K. Tischer, S. M. Reddy, and N. Osterrieder. 2001. Glycoproteins E and I of Marek's disease virus serotype 1 are essential for virus growth in cultured cells. *J. Virol.* **75**:11307–11318.
40. Smibert, C. A., B. Popova, P. Xiao, J. P. Capone, and J. R. Smiley. 1994. Herpes simplex virus VP16 forms a complex with the virion host shutoff protein vhs. *J. Virol.* **68**:2339–2346.
41. Sugimoto, K., M. Uema, H. Sagara, M. Tanaka, T. Sata, Y. Hashimoto, and Y. Kawaguchi. 2008. Simultaneous tracking of capsid, tegument, and envelope protein localization in living cells infected with triply fluorescent herpes simplex virus 1. *J. Virol.* **82**:5198–5211.
42. Vittone, V., E. Diefenbach, D. Triffett, M. W. Douglas, A. L. Cunningham, and R. J. Diefenbach. 2005. Determination of interactions between tegument proteins of herpes simplex virus type 1. *J. Virol.* **79**:9566–9571.
43. Wolfstein, A., C. H. Nagel, K. Radtke, K. Dohner, V. J. Allan, and B. Sodeik. 2006. The inner tegument promotes herpes simplex virus capsid motility along microtubules *in vitro*. *Traffic* **7**:227–237.